Paleobiology. 1976. vol. 2, pp. 316–331.

Hydrodynamic properties of cephalopod shell ornament

John A. Chamberlain, Jr. and Gerd E. G. Westermann

Abstract.—We investigated the hydrodynamic properties of cephalopod shell sculpture in two ways: 1) flow visualization experiments with sculptured shells; and 2) application of drag coefficient data for simple geometric bodies to cephalopod shells. Results of this work suggest:

1) the hydrodynamic effect of shell sculpture depends primarily on the size of the sculptural elements relative to the size of the shell and on the positions of sculpture elements on the shell and relative to each other.

2) sculpture is detrimental to swimming (reduces hydrodynamic efficiency) if it exceeds the height of the lower part of the shell's boundary layer.

3) sculpture is advantageous to swimming (increases efficiency) if it remains immersed in the boundary layer and induces premature conversion to turbulent boundary layer flow. To be hydrodynamically optimal, small shells (diam $\approx$ 10 cm) must have rough (sculptured) surfaces, whereas large shells (diam $\approx$ 100 cm) require smooth surfaces. Thus, in order to maintain maximum efficiency throughout life, the ontogeny of small individuals, or species, should be characterized by progressive roughening of the shell, while large forms should become increasingly smooth. Such allometries are observed among many ammonoids.

4) sculpture always has an effect on the flow around a cephalopod shell. In some species this effect was probably negligible, while in others, those with compressed shells especially, it was probably of major importance. In these species, sculpture appears to have functioned primarily to increase swimming ability.

John A. Chamberlain, Jr. Department of Geology, Brooklyn College of the City University of New York; Brooklyn, New York 11210

Gerd E. G. Westermann. Department of Geology, McMaster University; Hamilton, Ontario

Accepted: May 27, 1976

Introduction

Like all forms of locomotion, swimming is a process involving potentially great outlays of energy. One way that swimmers economize on propulsive energy expenditures is to maximize their hydrodynamic efficiency, i.e. the efficiency with which their limited muscle power is converted to velocity (Hertel 1966; Alexander 1968; Tucker 1975). This is accomplished by adopting body forms that minimize drag. Since little energy is lost accelerating the fluid (i.e. creating drag), the animal is in effect accelerated and can travel at higher velocity for a given power output. Two aspects of form are critical in minimizing drag: 1) body shape; and 2) surface roughness (Prandtl & Tietjens 1934; Hoerner 1965; Hertel 1966). Most swimmers have tapered, fusiform bodies and smooth, flexible surfaces. But because swimmers operate in different flow regimes, have different swimming capacities, and utilize different propulsion mechanisms, they exhibit a considerable range in these two properties.

The process of swimming in ectocochliate cephalopods (ammonoids and nautiloids) is constituted under the same physical principles controlling locomotion in all swimming animals (Chamberlain 1976). Thus, body shape and surface roughness can be expected to have been as critical in the adaptive scenario of most ectocochliates as in any other group of swimmers. Chamberlain (1971, 1973, 1976) has examined the effect of shape on the hydrodynamic efficiency of ectocochliates. His analysis shows that wide variation in hydrodynamic efficiency occurs as a function of variation in shell geometry and suggests that extension of the body of the animal behind the shell and variation in swimming attitude probably had little effect on hydrodynamic efficiency. However, relatively little attention has been given

to the hydrodynamic effect of surface roughness, i.e. shell ornamentation. Perhaps the only significant effort in this direction is that of Kummel & Lloyd (1955), who found, as one would expect, that the "relative drag coefficients" of coarsely ornamented shells were higher than those of smoother shells of approximately similar shape.

In this paper we examine the hydrodynamic properties of shell sculpture. We address ourselves to the following problems: 1) how does the pattern of fluid flow around an ornamented shell differ from that for a smooth shell; 2) what changes in hydrodynamic efficiency does sculpture produce; and 3) can sculpture be beneficial in swimming? Our present purpose is to erect a model for the hydrodynamic functioning of shell ornament. We want to establish a framework for further research in this area. We expect that additional work along the lines suggested here will help in clarifying the central issue of the adaptive significance of shell ornament. We hope that ultimately it will be possible to determine whether ornament primarily served some hydrodynamic function, for example to aid in swimming, or whether it served another single function, or whether it represents an adaptive compromise of a number of different functions.

Methods

Our method is one of analogy and experiment. We evaluate the probable hydrodynamic effect of shell ornament by drawing upon roughness data for simple geometric bodies. This approach is justified because flow patterns and drag coefficients of cephalopods are closely similar to those of blunt bodies (e.g. spheres, cylinders) and vary predictably from those of more elongated bodies (e.g. airfoils, ship hulls, ellipsoids) (Chamberlain 1976). Thus for the purpose at hand, we can expect the fluid dynamic behavior of shells to be adequately represented by these bodies. Chamberlain (1976) shows that for subcritical Reynolds numbers (i.e. Reynolds numbers less than about 5×10^5) this is in fact the case.

The experimental aspect of this work involves visualization of shell flow structure. Flow patterns for shells of nine ectocochliate species exhibiting various kinds of sculpture (see Table 1) were visualized using the method of dye injection described by Chamberlain (1976).

Although much can be learned about ectocochliate swimming performance by applying information gained from the experimental and analogic appoach taken here, drag coefficient tests of ornamented specimens are still necessary to evaluate the ideas raised here, and to provide more quantitative data on the hydrodynamic effect of shell ornament.

Flow Patterns of Ornamented Shells

Figure 1 shows flow patterns of a smooth-surfaced, plexiglas shell model (Figure 1A), and of shells of three of the species listed in Table 1 (Figure 1B–D). The three real shells exhibit different grades and kinds of roughness. *Zemistephanus* (Figure 1C) is very coarsely ornamented; *Skirroceras* (Figure 1D) is moderately ornamented; and *Nautilus* (Figure 1B) is virtually smooth. From Figure 1A, it is evident that a smooth shell surface produces flow characterized by: 1) attachment of the boundary layer to the leading part of the outer whorl; and 2) boundary layer separation along the lateral shoulder (see Chamberlain 1976). Where the boundary layer is attached, flow is directed backward and streamlines are undistorted. Turbulence occurs after the flow has separated. Chamberlain (1976) shows that this general pattern characterizes all smooth shells regardless of shell shape.

Fine growth lines, like those of *Nautilus* (Figure 1B), do not produce noticeable change in flow structure compared to the smooth model. The boundary layer separates at the lateral shoulder (although this is situated closer to the coiling axis in *Nautilus*). Boundary layer flow over the anterior part of the shell shows the same regularity as for the smooth model. Thus, it appears that shells having fine growth lines as their only ornament act as if they are effectively smooth surfaced, at least as far as overall flow structure is concerned. Figure 1C shows the effect of coarse ornament on flow structure. The coarse lateral spines of *Zemistephanus* disrupt the boundary layer by channelling the flow through topographic low areas of the shell's surface. Concentration of dye in the lee of these spines shows that large eddies form behind them. It is apparent that a much greater amount of turbulence is associated with this

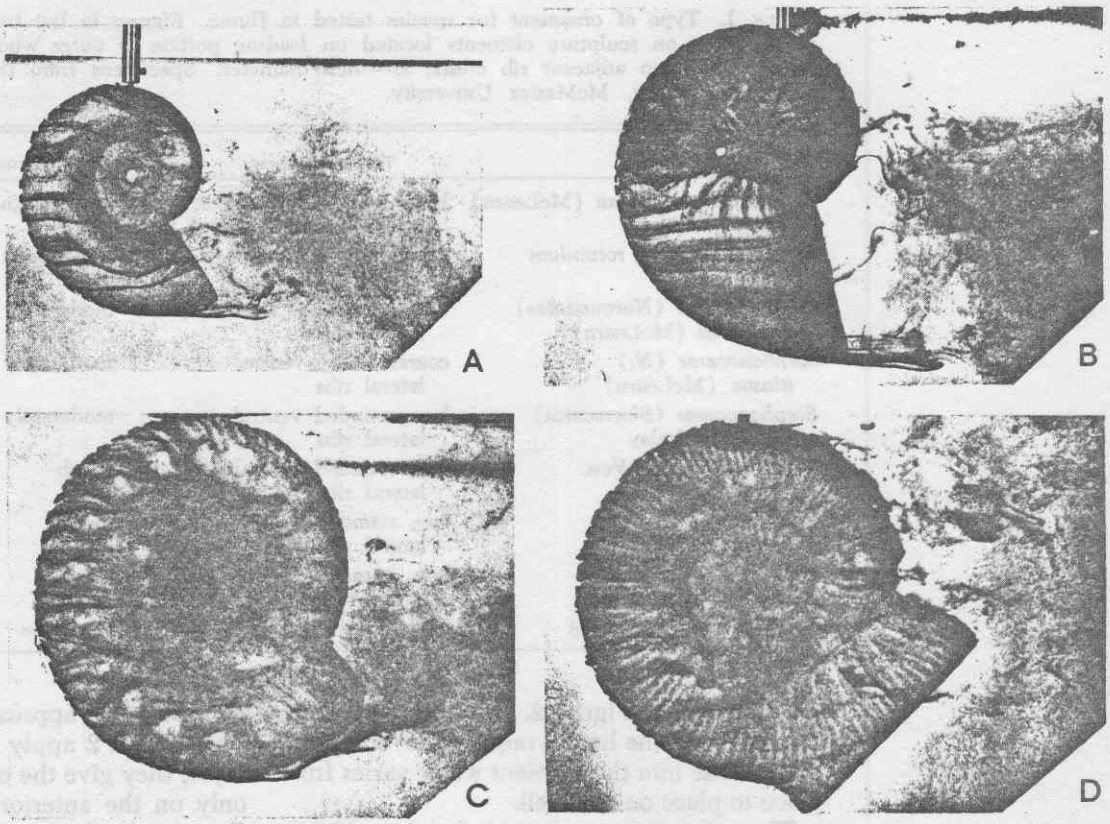

FIGURE 1. Flow patterns of smooth and ornamented shells. Separation is shown by distortion of dye streams along flank of outer whorl. Turbulence shown by swirls of dye in umbilicus and behind shell. Dark objects along venter are crystals of potassium permanganate. A, smooth surfaced shell model (from plate 84, fig. 1, of Chamberlain, 1976). B, *Nautilus*, fine growth lines (from plate 84, fig. 4, of Chamberlain 1976). C, *Zemistephanus*, coarse, lateral spines. D, *Skirroceras*, low, rounded, close-set ventral and lateral ribs.

type of flow pattern than with that of *Nautilus* or the smooth model. Figure 1D illustrates the effect of the close-set ribs of *Skirroceras*. This kind of ornament is representative of that found on many ammonoids and nautiloids. Comparison with Figure 1A and 1B shows that the basic character of the smooth surface flow pattern is preserved in *Skirroceras* although flow over the anterior part of the outer whorl is not quite so regular as in the smooth model and some channelling occurs.

Flow Structure and Sculpture Size

The effect of the grade of ornamentation on flow structure can be interpreted in terms of the nature of water motion near the surface of the shell. As for any body, the flow pattern of a cephalopod shell will be altered when surface roughness projects into water otherwise undisturbed by movement of the shell. In order to do this, sculpture must be large enough to extend through the envelope of moving water lying at the shell's surface and project into the ambient water outside. The thickness of this fluid shield varies across the surface of the shell. Where flow is attached, the envelope corresponds approximately to the lower third of the boundary layer (displacement layer), but where separation has occurred, it becomes the stagnant region above the umbilicus (which is actually part of the wake—see Chamberlain 1976). We assume here that the average velocity in the wake near the shell is essentially equal to that of the shell. This is the case for other blunt bodies (Prandtl and Tietjens 1934; Hoerner 1965). The relationship of these flow regions to the shell is

TABLE 1. Type of ornament for species tested in flume. Figures in last two columns refer to measurements taken on sculpture elements located on leading portion of outer whorl only. K—rib height; λ—distance between adjacent rib crests; D—shell diameter. Specimens from the collection of the Department of Geology, McMaster University.

Species	Type of ornament	Grade of ornament	Relative shape (K/λ)	Relative size (K/D)
Zemistephanus itinsae (McLearn)	large lateral ribs, spines; coarse rounded ventral ribs	very rough	.33	.060
Megasphaeroceras rotundum Imlay	coarse, sharp ventral + lateral ribs	very rough	.36	.034
Stephanoceras (*Normannites*) *crickmayi* (McLearn)	coarse, rounded ventral + lateral ribs	moderately rough	.22	.021
Stephanoceras (*N.*) *itinsae* (McLearn)	coarse, sharp ventral + lateral ribs	moderately rough	.32	.019
Stephanoceras (*Skirroceras*) *kirschneri* Imlay	low, rounded ventral + lateral ribs	moderately rough	.20	.010
Tmetoceras kirki West.	low, rounded ventral + lateral ribs	rough	.14	.009
Hammatoceras lotharingicum Ben.	low, rounded ventral + lateral ribs; small keel	rough	.14	.009
Abbasites abbas Buck.	low, rounded ventral + lateral ribs	rough	.17	.008
Nautilus pompilius Liné	fine growth lines	very fine	—	.0001

diagrammed in Figure 2. It is apparent from Figure 2 that the height required for sculpture to protrude into the ambient water varies from place to place on the shell.

The minimum, or critical, height which a sculpture element must attain in order to emerge from the displacement layer may be estimated from the equations for boundary layer thickness of a flat plate. Using Hertel's (1966) expressions for boundary layer thickness, we find:

$$\delta_L^* = 5L_s/R_e^{1/2} \quad (1)$$

$$\delta_T^* = 0.36L_s/R_e^{1/5} \quad (2)$$

where δ_L^* is displacement layer thickness of a laminar boundary layer; δ_T^* is the displacement layer thickness of a turbulent boundary layer; L_s is the distance of the sculpture element from the leading edge of the shell; and R_e is Reynolds number. Reynolds number of any sculpture element may be found from:

$$R_e = VL_s/\nu \quad (3)$$

where V is velocity of the shell; and ν is kinematic viscosity of the fluid ($\nu = 10^{-2}\text{cm}^2/\text{sec}$ for sea water under normal temperature-salinity conditions). Equation 1 applies when the boundary layer is laminar ($R_e < 5 \times 10^5$ approximately), while equation 2 is to be used when the boundary layer becomes turbulent ($R_e < 5 \times 10^5$ approximately). Because equations 1 and 2 apply to an attached boundary layer, they give the critical height of sculpture only on the anterior part of the shell where flow is attached.

It is apparent from equations 1–3 that where the boundary layer is attached, critical height increases backwards from the leading edge of the shell and decreases with increasing velocity. Anterior sculpture elements which are large enough to generate drag at one position on a shell may have no effect at another. Likewise, high swimming velocities may expose sculpture which at lower velocities is immersed in the boundary layer. This may be seen in Figure 3, which shows how displacement layer thickness (δ^*) varies with velocity (V) and position (L_s). When $V = 10$ cm/sec, for example, δ^* increases backward from the leading edge ($L_s = 0$). When $V = 100$ cm/sec, the same trend is observed, but δ^* is less for a given L_s than when $V = 10$ cm/sec, and a significant drop in δ^* occurs when the flow becomes turbulent (at $L_s \sim 50$ cm). Figure 3 shows that in the probable velocity range of ectocochliates (10–100 cm/sec, approximately as we describe below), displacement layers are normally very thin—a few millimeters at most. Only the finest growth lines, like those of *Nautilus* would remain entirely within the

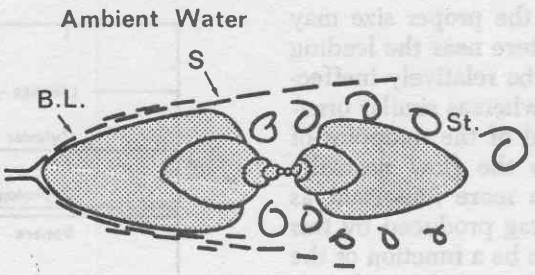

FIGURE 2. Water motion near surface of shell. S—separation point. B.L.—attached boundary layer. St.—stagnant wake behind separation point.

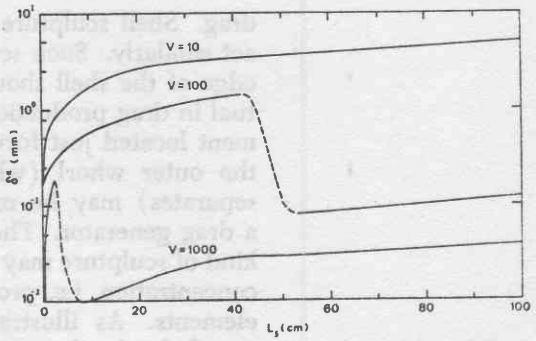

FIGURE 3. Estimated displacement thickness of an attached boundary layer as a function of velocity and position of sculpture on shell. δ^*—displacement layer thickness. L_s—distance of sculpture from leading edge of shell. V—velocity in cm/sec. Sharp decrease in curves for V = 100 cm/sec and V = 1000 cm/sec, is due to conversion from laminar to turbulent boundary layer flow.

displacement layer over this velocity range, and thus have little effect on flow structure. In contrast, coarse sculpture, such as that of *Zemistephanus* would emerge from the displacement layer over virtually all of this velocity range, and cause the major disruption shown in Figure 1C. Sculpture having dimensions intermediate to these extremes, like that characterizing the other species tested, would be covered or emergent depending on velocity and position.

When separation occurs the boundary layer leaves the surface of the shell creating a thick dead-water region at the surface, as diagrammed in Figure 2. Sculpture situated behind the point of separation must therefore be much larger than sculpture located in front of the separation point in order to penetrate into normally undisturbed, ambient water. In fact, the wake is normally so extensive that all but unusually coarse sculpture will remain immersed in it. Note that the spines of *Zemistephanus* (Figure 1C) do not seem to have much effect on the flow once separation has occurred. Except when ornament is uncommonly prominent, sculpture located behind the point of separation probably is virtually inoperative in the hydrodynamic sense. For many types of shells, evolute and depressed forms especially, this means that most of the shell's ornament probably has little effect on flow structure. Spines and ribs in the interior of the umbilicus, along the umbilical wall, and on the trailing portion of the outer whorl should therefore have little hydrodynamic significance. Normally, only sculpture on the leading part (with respect to swimming direction) of the outer whorl—the part of the shell to which the boundary layer is attached—would significantly influence flow structure. In this context, it is of interest to note that in many species, the most prominent ribs are placed behind the lateral shoulder where they would have the least effect on the flow.

Sculpture Drag

Although more detailed analysis than we attempt here is needed to document the nature of the relationship between sculpture and drag, it seems clear that the drag of a rib or spine should be roughly proportional to the degree to which it extends above the boundary layer. Sculpture protruding a short distance above the boundary layer should generate only minor disturbances and probably induce little additional drag. Coarse sculpture, such as that of *Zemistephanus*, should augment drag considerably. In many cases, sculpture drag probably exceeds shell drag (drag due to shell alone, i.e. without sculpture), particularly where shell drag is low (e.g. in oxycones—see Chamberlain 1976).

If sculpture does not greatly exceed the height of the boundary layer, sculpture drag may also depend on the distribution of individual sculpture elements. For spheres, the effect of surface roughness having dimensions approximately equivalent to boundary layer thickness varies with position. Roughness carried anteriorly causes only small local flow disturbances, while further back near the sphere's equator, it causes premature flow separation, and results in this case in a large increase in

drag. Shell sculpture of the proper size may act similarly. Such sculpture near the leading edge of the shell should be relatively ineffectual in drag production, whereas similar ornament located just forward of the midpoint of the outer whorl (where the flow normally separates) may be much more important as a drag generator. The drag produced by this kind of sculpture may also be a function of the concentration, i.e. proximity, of the sculpture elements. As illustrated in Figure 1D, the rounded, closely spaced ribs of *Skirroceras* permit the smooth shell flow pattern to develop. The ribs are apparently close enough to permit the boundary layer to flow along the rib crests with only small diversions into the inter-rib troughs or little tendency to completely separate from the shell. Because premature separation is inhibited, this kind of rib configuration would seem to diminish sculpture drag over that of more distantly spaced but equally sized ribs. The situation in cephalopod shells is probably analagous to that of spheres and airfoils wherein the effectiveness of surface roughness first increases with increasing concentration (as the number of individual elements increases) and then decreases at higher concentrations (as the elements become more closely spaced). A shell with only a few ribs would thus appear to be at a disadvantage with respect to hydrodynamic efficiency compared to a shell having many closely spaced ribs of equal size.

In any shell the significance of the sculpture drag component should depend to some extent on shell drag. In cases where shell drag is large, as in depressed shells (Chamberlain 1976), a prominent sculpture component would be required to induce marked gains in total drag. But where shell drag is low, as in many oxycones, even small sculpture drag additions would be large in comparison to that produced by the shell. As a result, low drag shells are undoubtedly much more sensitive to the hydrodynamic consequences of roughened surfaces.

Boundary Layer Conversion

Figure 4 shows that for blunt, rounded bodies, like cephalopod shells, reduction in drag coefficient can accompany conversion from laminar to turbulent boundary layer flow. Consider what this might mean to an ammonoid or nautiloid. If it could swim fast enough or grow large enough to attain the critical Reynolds number for conversion ($R_e \propto V \cdot \text{Size}$), and thereby cause the flow to convert, its hydrodynamic efficiency could be increased markedly, perhaps by as much as an order of magnitude (streamlining does not increase since no change in shell shape is involved). Such gains in energy economy rival those due to gross change in morphology and thus may have been of the utmost importance in the swimming mechanics of fossil cephalopods.

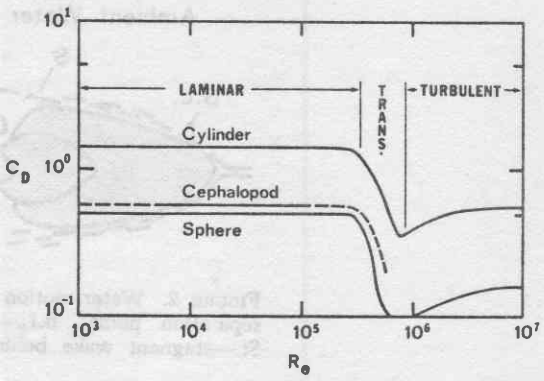

FIGURE 4. Effect of boundary layer transition on drag coefficient of some blunt bodies (after text-figure 6A, of Chamberlain 1976). C_D—drag coefficient. R_e—Reynolds number.

It is well known that critical Reynolds number is not constant but varies as a function of body shape and surface roughness. Thus it is conceivable that shell ornament may have been used as a means of ensuring turbulence in the boundary layer and a relatively high hydrodynamic efficiency. We examine this idea in the following paragraphs. Since boundary layer conversion depends on body shape as well as surface roughness, we find it necessary to deal with both factors in this analysis. We first estimate the velocity required to produce transition for smooth cephalopod shells of various shapes and sizes and then show how the addition of sculpture effects these velocities.

The Effect of Shape

The effect of body shape on critical Reynolds number and drag coefficient is shown in Figure 5 for smooth bodies having various shapes (where shape is expressed as fineness ratio, or maximum width/maximum length).

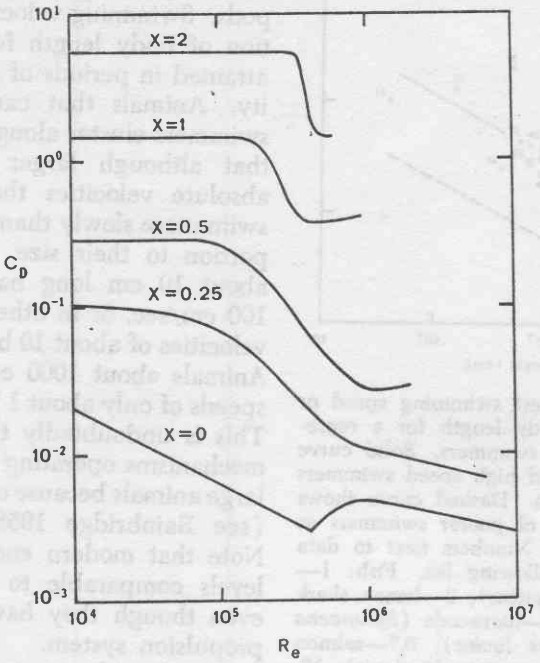

FIGURE 5. Effect of body shape on critical Reynolds number for smooth, streamlined struts. X—fineness ratio (body width/body length). C_D—drag coefficient. R_e—Reynolds number. Curve for X = 0, for frictional drag of a flat plate held parallel to the flow. After figure 6–2 of Hoerner 1965.

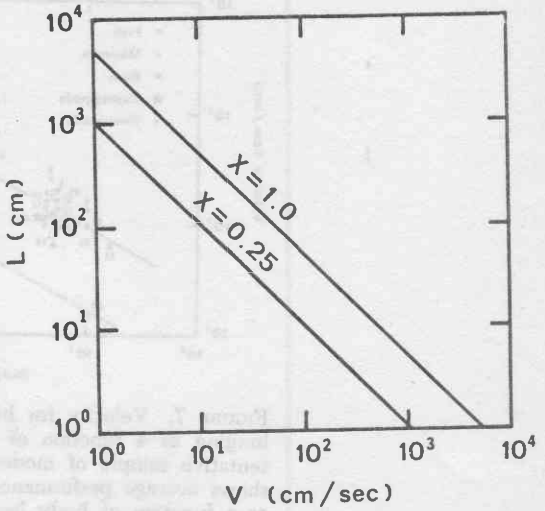

FIGURE 6. Estimated critical size (L) and velocity (V) required to produce transition. Diagonals represent conversion thresholds. X—fineness ratio. X = 0.25, compressed shells. X = 1.0, depressed shells. See text for further explanation.

It is apparent that as fineness ratio (X) decreases (body shape becomes more elongate), critical Reynolds number decreases by a factor of about five in the fineness ratio range of cephalopod shells ($X > 0.1$ approximately). In order to achieve laminar-turbulent transition, compressed shells ($X \approx 0.25$) would probably require only about one fifth the velocity of depressed shells ($X \approx 1.0$) of equal size (equal shell diameter). Transition and its attendant hydrodynamic advantages would thus seem to be more easily attainable to cephalopods having compressed shells. Undoubtedly, umbilical dimensions are of some importance because in forcing early separation, even on shells with fairly small X, wide umbilici cause shells to act as if they were "thicker" than they actually are (Chamberlain 1976). Figure 5 also shows that the gain in efficiency (drop in drag coefficient) associated with transition is more abrupt, and therefore perhaps potentially more useful, when shells are depressed. At very low fineness ratios ($X < 0.1$ approximately), the decrease in drag coefficient becomes progressively less pronounced so that overly compressed shells would gain little by conversion, and could perhaps suffer the transition related drag increase of highly flattened bodies.

When critical Reynolds number and body size are known, equation 3 can be used to obtain the velocity necessary for conversion. Figure 6 is a plot of this critical velocity versus size (shell diameter) for smooth shells. In order to induce conversion, a given shell must have a size-velocity product sufficient to produce the critical Reynolds number for its fineness ratio. The required values plot as diagonal lines, or conversion thresholds, in Figure 6. A shell will produce conversion if its size-velocity product lies on or above the conversion threshold for its fineness ratio. Thus, critical velocities for compressed shells will be clustered along the diagonal line labelled $X = 0.25$ in Figure 6, while critical velocities for depressed shells should lie near the line marked $X = 1.0$. Critical velocities for most other shells should be intermediate to these extremes.

Figure 6 tells us how fast a smooth cephalopod of a given size and shape must travel in order to induce transition, but it does not tell us whether a particular animal could actually travel at the required speed. For this we need to know the swimming speed of the animal in

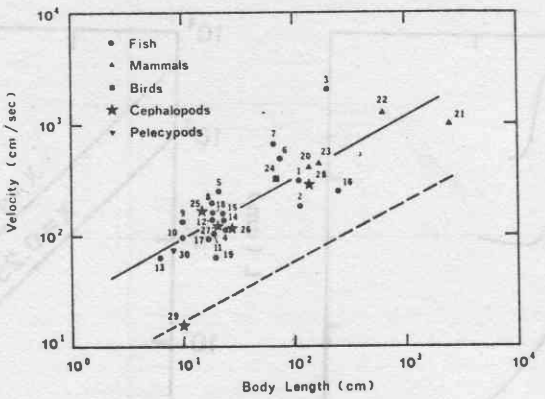

FIGURE 7. Velocity for highest swimming speed or lunging as a function of body length for a representative sample of modern swimmers. Solid curve shows average performance of high speed swimmers as a function of body length. Dashed curve shows probable performance levels of poorer swimmers as a function of body length. Numbers next to data points identify species in following list. Fish: 1—white shark (*Carcharhinus leucas*); 2—lemon shark (*Negarprion brevirostris*); 3—barracuda (*Sphyraena barracuda*); 4,5—pike (*Esox lucius*); 6,7—salmon (*Salmo salar*); 8,9—dace (*Leuciscus leuciscus*); 10, 11—trout (*Salmo irideus*); 12,13—goldfish (*Carassius auratus*); 14—rudd (*Scardinius erythrophthalmus*); 15—alewife (*Parolobus pseudoharengus*); 16—sailfish (*Istiophorus* sp.); 17—herring (*Clupea harengus*); 18—sea trout (*Salmo trutta*); 19—bream (*Abramis brama*). Mammals: 20—porpoise (*Tursiops gilli*); 21—blue whale (*Balaenoptera musculus*); 22—killer whale (*Orcinus orca*). 23—sea lion (*Zalophus californianus*). Birds: 24—penguin (*Spheniscus humboldti*). Cephalopods: 25—squid (*Loligo vulgaris*), backward; 26—squid (*Loligo vulgaris*), forward; 27—squid (*Loligo pealii*), backward; 28—squid (*Dosidicus gigas*), backward; 29—*Nautilus pompilius*, backward. Pelecypods: 30—scallop (*Placopecten magellanicus*). References: fish—Stringham (1924), Magnan (1930), Gero (1952), Gray (1957), Bainbridge (1960); mammals—Johannessen and Harder (1960), Lang and Norris (1966); cephalopods—Packard (1969), Cole and Gilbert (1970); Pelecypods—Caddy (1968). Figures for sea lion and penguin based on speed-size estimates made by J.A.C. on captive animals swimming in enclosed pens in Detroit and Philadelphia zoos and New York City Aquarium. Figures for *Nautilus* based on speed-size estimates made by J.A.C. from Jacques Cousteau television film.

question. Unfortunately, virtually nothing is presently known about the swimming speed of fossil cephalopods. However, performance data for modern swimmers can be used to estimate the probable limits of swimming speed in the fossils. Figure 7 shows such data for a representative group of modern swimmers including *Nautilus* and several other cephalopods. Swimming velocity is plotted as a function of body length for the highest velocity attained in periods of peak locomotory activity. Animals that can be considered good swimmers cluster along the solid line. We see that although larger animals have higher absolute velocities than smaller ones, they swim more slowly than smaller animals in proportion to their size. For example, animals about 10 cm long have velocities of about 100 cm/sec, or in other words, they travel at velocities of about 10 body lengths per second. Animals about 1000 cm long, however, have speeds of only about 1 body length per second. This is undoubtedly the result of propulsion mechanisms operating at lower frequencies in large animals because of adverse scaling effects (see Bainbridge 1958, 1960; Hertel 1966). Note that modern endocochliates perform at levels comparable to other good swimmers, even though they have a radically different propulsion system.

Nautilus (data point 29 in Figure 7), however, apparently represents a different situation—one which illustrates very clearly the problems that can arise when morphology must simultaneously satisfy two antithetical adaptive needs. Buoyancy regulation in *Nautilus*, as in other ectocochliates, is accomplished by giving over a large portion of the total volume of the animal to gas-filled space devoid of tissue (phragmocone), the primary function of which is to neutralize the weight of the shell. But the need to maintain the phragmocone as a buoyancy device has the effect of reducing the body space available for propulsive muscle. As a result, *Nautilus* has much less propulsive muscle relative to its mass than do modern swimmers (in which propulsive musculature may exceed 50% of total body mass, Bainbridge 1960). *Nautilus* is therefore a much less powerful swimmer than the other animals included in Figure 7. Also, the hydrodynamic efficiency of *Nautilus* is nearly an order of magnitude less than for well streamlined, fusiform animals like the good swimmers in Figure 7 (see Chamberlain 1976). These two factors combine to make *Nautilus* a comparatively poor swimmer in the absolute sense, although for an ectocochliate it probably is a relatively good swimmer (see Chamberlain 1976). Since the same scaling laws apply to all

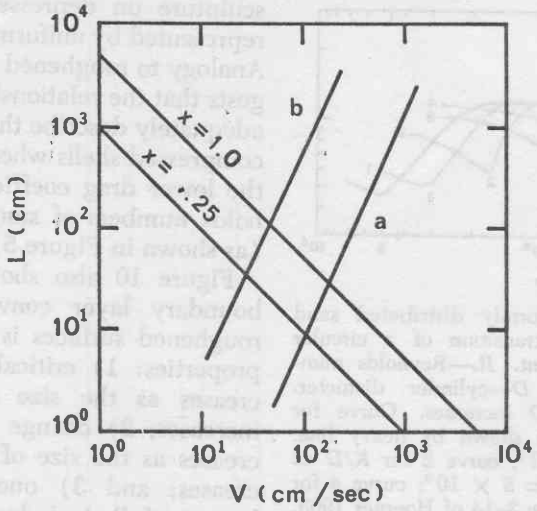

FIGURE 8. Estimated critical velocity (V) and length (L) for fossil cephalopods having different levels of swimming performance. Curve a for animals with performance levels similar to that of *Nautilus*. Curve b for animals with performance levels similar to that for modern rapid swimmers. Most fossil cephalopods probably fall along or above curve a. See text for further explanation.

swimmers, it follows that the effect of size on swimming velocity for swimmers comparable to *Nautilus* should be roughly similar to that sketched by the dashed line in Figure 7.

Fossil ectocochliates were similar to *Nautilus* in overall anatomy as shown in the reconstructions of ectocochliate anatomy given by Mutvei (1957, 1964), Jordan (1968), and Lehmann (1971, 1972). In particular, they had large phragmocones and relatively poorly streamlined shells. We can thus expect that their performance should be adequately represented by that of *Nautilus*. We can therefore use the dashed line in Figure 7 as a general rule to relate maximum swimming velocity to shell size in fossil ectocochliates. Since fossil cephalopods certainly could have performed no better than modern swimmers, we may use the solid curve to set an upper limit on fossil ectocochliate performance.

Figure 8 shows these two performance curves superimposed upon the size-velocity plot in Figure 6. Curve a, is for the modern good swimmers; curve b, is for *Nautilus* performance levels. Since these performance curves indicate velocities attained by animals of a given size, their intersections with the diagonals give the minimum shell size required

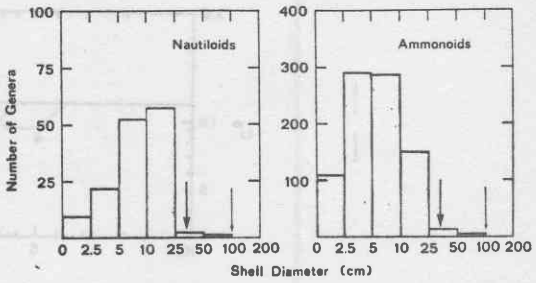

FIGURE 9. Size-frequency plot of shell diameter for planispirally coiled ectocochliates. Arrows show minimum size necessary to induce transition assuming performance equal to *Nautilus*. Thick arrows for compressed shells; thin arrows for depressed shells. Size data are from descriptions of genera illustrated in the nautiloid and ammonoid volumes of the Treatise on Invertebrate Paleontology. Total sample size: nautiloids—142 genera; ammonoids—843 genera.

to produce transition. For example, suppose a certain fossil ectocochliate had the same performance capabilities and drag coefficient as *Nautilus*. If its shell were 10 cm in diameter, then it would have a maximum velocity of about 25 cm/sec, far too low to induce transition. As suggested in Figure 8, the shell would have to be about 40 cm in diameter if it were compressed and about 100 cm in diameter if it were depressed in order to induce transition. We assume here that drag coefficient differences between *Nautilus* and these other types of shells do not greatly alter performance levels. Poorer swimmers would require correspondingly larger shells, and better swimmers correspondingly smaller shells. Chamberlain's (1976) data on shell drag coefficients implies that *Nautilus* was probably a fairly good swimmer for an ectocochliate, so that there is little likelihood that species with shells much smaller than that of *Nautilus* could achieve transition (*Nautilus* probably can't). If they were smooth, most fossil cephalopods would probably require shells much larger than *Nautilus* in order to induce transition. Figure 8 suggests 30–40 cm as a necessary minimum. Since most species had shells smaller than this (see Figure 9), it appears that if shells were smooth surfaced, only the very largest species could probably achieve transition. The hydrodynamic advantage of a turbulent boundary layer would probably escape the great majority of ectocochliates. We would point out that the *Treatise* size data (upon which Figure 9

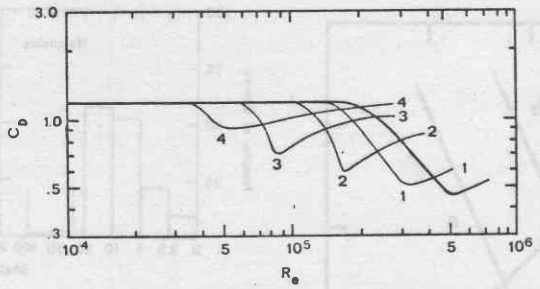

FIGURE 10. Effect of uniformly distributed sand grains on boundary layer transition of a circular cylinder. C_D—drag coefficient. R_e—Reynolds number. K—grain diameter. D—cylinder diameter. Roughness increases as K/D increases. Curve for smooth surface ($K/D = 0$) shown by heavy line. Curve 1 for $K/D = 5 \times 10^{-4}$; curve 2 for $K/D = 2 \times 10^{-3}$; curve 3 for $K/D = 5 \times 10^{-3}$; curve 4 for $K/D = 2 \times 10^{-2}$. After figure 3–14 of Hoerner 1965.

is based) may tend to be too low because very large specimens are rarely figured in the literature. This, however, should not greatly affect our argument.

The Effect of Sculpture

Experiment has shown that roughened surfaces can induce flow conversion at unusually low Reynolds numbers (see Prandtl & Tietjens 1934; Hoerner 1965; Hertel 1966). Shell sculpture may therefore enable many ectocochliates to capitalize upon drag coefficient changes associated with conversion by bringing these changes within their normal velocity range. However, experiment also shows that in order to act in this way roughness elements must be small enough to remain immersed in the boundary layer. Sculpture should be similarly fashioned if it is to be of similar benefit to its bearer.

We can obtain an idea of the consequenses of such sculpture by considering the effect of surface roughness of simple geometric bodies like cylinders. Figure 10 is a plot of drag coefficient against Reynolds number for cylinders having several different degrees of roughness. The roughness data are for sand grains distributed uniformly over the cylinder surface and do not, therefore, exactly correspond to the ordered kinds of roughness found in cephalopod shells. For our purposes, however, this difference should not lead to major difficulties, and we will assume that the effect of sculpture on depressed shells is adequately represented by uniformly roughened cylinders. Analogy to roughened streamlined bodies suggests that the relationships shown in Figure 10 adequately describe the effect of roughness on compressed shells when allowance is made for the lower drag coefficients and critical Reynolds numbers of smooth streamlined bodies (as shown in Figure 5).

Figure 10 also shows that the premature boundary layer conversion associated with roughened surfaces is characterized by three properties: 1) critical Reynolds number decreases as the size of roughness elements increases; 2) change in drag coefficient decreases as the size of roughness elements increases; and 3) once the boundary layer becomes fully turbulent, smooth surfaces again produce lower drag coefficients. Thus, boundary layer conversion results in little hydrodynamic advantage if roughness is too large (insignificant reduction in drag coefficient), or too small (insignificant reduction in critical Reynolds number), and is detrimental if Reynolds number is too high. Cephalopod sculpture should probably lie within the limits shown in Figure 10 ($5 \times 10^{-4} \leq K/D \leq 2 \times 10^{-2}$) to produce favorable results (where K for cephalopods can be taken as the amplitude or height of the ribs, and D as shell diameter). Relative rib size (K/D) for the specimens discussed in this paper is given in Table 1. Since the advantage gained in conversion is a temporary one, cephalopods with rough surfaces must operate at velocities producing Reynolds numbers less than about 5×10^5. Thus boundary layer conversion is of limited use. It can greatly augment energy economy only within a limited velocity range. But as long as an animal operates within these limits, it represents a valuable means for economizing on energy expenditures.

One result of the lower critical Reynolds number brought about by shell sculpture of the proper size (see Figure 10) is reduction in critical velocity. To produce conversion, a sculptured cephalopod would not need to travel as fast as a smooth one. Thus, sculpture may act to bring conversion within an animal's velocity range. We can explore this idea by considering how critical velocity and critical size are affected by surface roughness. Figure 11 illustrates this effect for depressed (Figure

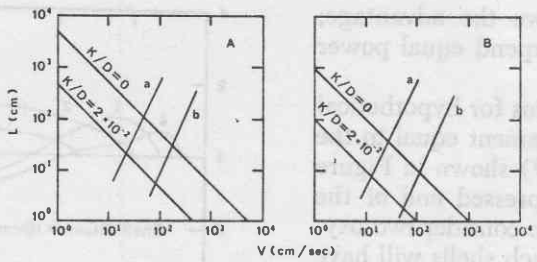

FIGURE 11. Estimated critical velocities and lengths for fossil cephalopods having roughened surfaces. A, for depressed shells (X = 1.0). B, for compressed shells (X = 0.25). Diagonal line labelled ($K/D = 0$) is the conversion threshold for smooth shells. Diagonal line labelled 2×10^{-2} is the conversion threshold for rough shells. Curve a for *Nautilus* performance level. Curve b for performance level of modern rapid swimmers.

11A) and compressed (Figure 11B) shells. The diagonal lines show conversion thresholds for smooth shells ($K/D = 0$) and rough shells ($K/D = 2 \times 10^{-2}$). Performance curves for *Nautilus* and modern good swimmers are shown by lines a and b respectively. We see that in the case of depressed shells, critical size decreases from about 100 cm to about 40 cm (assuming *Nautilus* performance levels), and from about 40 cm to about 10 cm in compressed shells (again, assuming *Nautilus* performance levels). Thus, critical size reduction resulting from sculpture of the proper kind appears sufficient to enable many more species to achieve transition, as suggested in the size distribution of ectocochliate species (Figure 9). This is especially so for species with compressed shells, but it is still unlikely that significant numbers of species with depressed shells could attain transition. Although lesser grades of roughness will result in higher critical sizes than for $K/D = 2 \times 10^{-2}$, it is nevertheless apparent that shell sculpture could be essential to many species, especially those with compressed shells, in bringing conversion within their performance capabilities.

The effect of boundary layer conversion on swimming performance can be estimated by calculating the propulsive power required to produce a given velocity during sustained swimming for rough and smooth shells. The power required to produce motion at a constant speed is:

$$P = F\,V \tag{4}$$

where P is power; F is force or thrust of the propulsive muscles; and V is velocity. Since propulsive force must equal drag force when velocity is constant (Σ forces $= 0$, in motion at constant velocity; Newton's first law), we can write:

$$F = D_F = \tfrac{1}{2}\,\rho\,V^2\,A\,C_D$$

where D_F is drag force; ρ is the density of seawater; A is an area representative of the shell; and C_D is shell drag coefficient. Substituting into equation 4, we obtain:

$$P = \tfrac{1}{2}\,\rho\,V^3\,A\,C_D \tag{5}$$

It is convenient to evaluate power output of smooth and rough shelled animals in the form of a power ratio defined as:

$$P.R. = P_s/P_r \tag{6}$$

where $P.R.$ is the power ratio; P_s is the power required to produce a given velocity for a smooth shell; and P_r is the power required to produce that same velocity in an ornamented shell of equal size and shape. Thus, from equations 5 and 6:

$$P.R. = [(\tfrac{1}{2}\rho V^3 A C_{D_s})/(\tfrac{1}{2}\rho V^3 A C_{D_r})] \tag{7}$$

where C_{D_s} is the drag coefficient of the smooth shell; and C_{D_r} is the drag coefficient of the ornamented shell. Cancelling, we have:

$$P.R. = C_{D_s}/C_{D_r}. \tag{8}$$

C_{D_s} and C_{D_r} can be found from data such as that shown in Figure 10 (of course, the drag coefficient data must pertain to the body in question). For example, suppose we wanted to obtain $P.R.$ for a cylinder 10 cm in diameter having a roughness of $K/D = 2 \times 10^{-2}$, and travelling at 50 cm/sec. The Reynolds number for this situation is $R_e = 5 \times 10^4$ ($R_e = V \cdot L \cdot 10^2 = 50 \cdot 10 \cdot 100 = 5 \times 10^4$). From Figure 10, C_{D_s} at $R_e = 5 \times 10^4$ is 1.2, and C_{D_r} is 0.9. Thus $P.R. = 1.333$.

The significance of our power ratio is that it tells us which body requires more power to travel at some given velocity. In the above example, the rough cylinder is the more economical because it requires 25% less power [(1.333 – 1)/1.333 = .25] than the smooth one. In the case of cephalopods, our power ratio shows which kind of shell is more efficient. When $P.R. > 1$, ornamented shells require less power and are adaptively advantageous; when

$P.R. < 1$, smooth shells have the advantage; and when $P.R. = 1$, both expend equal power and are equally efficient.

We calculated power ratios for hypothetical shells having grades of ornament equal to the degrees of roughness (K/D) shown in Figure 10. To represent the compressed end of the morphological spectrum, we consider two oxyconic shells ($X = 0.25$). Such shells will have $C_{D_s} \approx 0.2$ as discussed by Chamberlain 1976. C_{D_r} can be estimated from the cylinder data in Figure 10 by using $C_{D_s} = 0.2$ for sub-critical Reynolds numbers instead of $C_{D_s} = 1.2$ and adjusting the shape of the C_D–R_e curves to conform to that for bodies with $X = 0.25$, as estimated from Figure 5. We consider two such shells—a small one (diameter = 10 cm, which our previous arguments suggest as just large enough to induce transition; and a large one (diameter = 100 cm). We also consider two depressed shells ($X = 1.0$)—one having a diameter of 40 cm (smaller animals were probably unable to induce transition) and one with a diameter of 100 cm. Chamberlain's (1976) analysis of shell drag coefficient suggests a typical shell of this morphology should have $C_{D_s} \approx 0.8$. C_{D_r} can be estimated as outlined above.

Results for the compressed shells are shown in Figure 12. For the 10 cm shell, addition of shell ornament should result in considerable saving of energy (> 50%) above velocities of about 15 cm/sec. Assuming *Nautilus* performance levels (i.e. $V \approx 20$ cm/sec, from Figure 7) the optimum sculpture size is $K/D = 2 \times 10^{-2}$ (curve 4 in Figure 12A). Finer sculpture will not produce transition at these velocities, and therefore would be hydrodynamically useless. Acounting for the C_D difference between *Nautilus* and our hypothetical oxycones (C_D = 0.2, versus 0.5 for *Nautilus*, see Chamberlain 1976), and assuming that the energy saved by the lower C_D in compressed shells is put into higher velocity (i.e. raising V to about 30–40 cm/sec), we can see that the optimum shell ornament still is $K/D = 2 \times 10^{-2}$. Even if we assume a performance level comparable to modern swimmers (i.e. $V \approx 100$ cm/sec), a rough surface is still advantageous, although the optimum grade of ornament reduces to $K/D = 2 \times 10^{-3}$ (curve 2 in Figure 12A). For the 100 cm shell, the optimum surface depends on velocity. At velocities below about 100 cm/sec, a slightly roughened surface is most economical, but above this limit, a smooth surface becomes advantageous. Assuming *Nautilus* performance levels (i.e. $V \approx 50$–70 cm/sec, from Figure 7) very fine sculpture ($K/D = 5 \times 10^{-4}$) is optimal (curve 1 in Figure 12B). However, if we account for C_D differences between *Nautilus* and compressed shells as above (i.e. V increases to more than 100 cm/sec) then it becomes evident that smooth shells are hydrodynamically optimal.

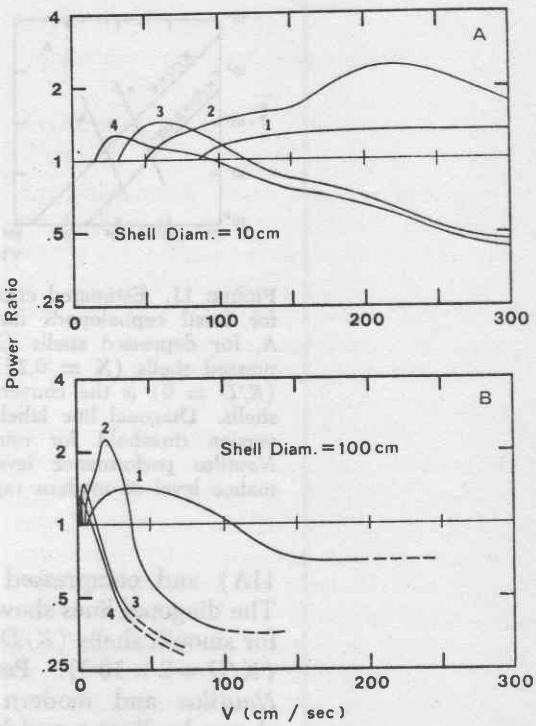

FIGURE 12. Calculated power ratios for cephalopods with smooth and ornamented, compressed shells (X = 0.25) as a function of swimming velocity (V) and shell diameter. A, for shell diameter = 10 cm. B, for shell diameter = 100 cm. Power ratio (P.R.) —ratio of power output of smooth to ornamented shell. When P.R. > 1, ornamented shell requires less power to maintain a given velocity than rough shell. When P.R. < 1, ornamented shell requires more power. When P.R. = 1, ornamented and smooth shell require same power. Each curve is for a different grade of ornamentation: curve 1—$K/D = 5 \times 10^{-4}$; curve 2—$K/D = 2 \times 10^{-3}$; curve 3—$K/D = 5 \times 10^{-3}$; curve 4—$K/D = 2 \times 10^{-2}$.

Results for the hypothetical depressed shells are shown in Figure 13. Comparison with Figure 12 shows that the effect of ornament is comparable for both types of shells—rough surfaces are advantageous at low velocities,

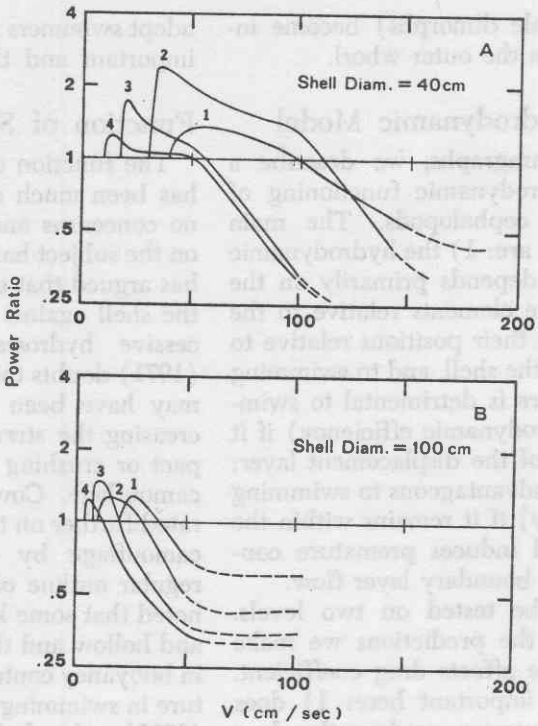

FIGURE 13. Calculated power ratios (P.R.) for cephalopods with smooth and ornamented, depressed shells ($X = 1.0$) as a function of swimming velocity (V) and shell diameter. A, for shell diameter = 40 cm. B, for shell diameter = 100 cm. Each curve is for a different grade of roughness: curve 1—$K/D = 5 \times 10^{-4}$; curve 2—$K/D = 2 \times 10^{-3}$; curve 3—$K/D = 5 \times 10^{-3}$; curve 4—$K/D = 2 \times 10^{-2}$.

while smooth surfaces excel at higher velocities. Assuming *Nautilus* performance levels, sculpture having $K/D = 2 \times 10^{-3}$ is optimal for the smaller shell, while for the 100 cm shell, a smooth surface is optimal. Similar results are obtained when allowing for C_D differences between depressed shells and *Nautilus* as in the previous example.

We would emphasize that our treatment of sculpture power ratios contains several assumptions about the behavior of sculpture drag coefficients (C_{D_r}) as a function of Reynolds number. While these assumptions may affect the numerical results of our calculations, they should not detract from the biological validity of our arguments. We would also point out that our use of generalized, hypothetical shells implies that the calculated values may not strictly apply to many real shells, especially those having shell shapes different from the shapes we consider here.

Implications for Ectocochliate Growth

Our observations on the effect of sculpture on boundary layer flow lead us to consider the significance of sculpture in the ontogenetic development of ectocochliates. From Figures 12 and 13, it is evident that for both compressed and depressed shells, but particularly the former, change in grade of ornament should accompany size increase in order to maintain the greatest possible hydrodynamic efficiency. For example, compressed species with adult sizes of about 100 cm should become progressively smoother during growth. Being smaller, juveniles of such species would be favored if they had fairly rough shells ($K/D \approx 2 \times 10^{-2}$ at about 10 cm), but with increasing size, the advantage swings toward smoother shells ($K/D \approx 5 \times 10^{-4}$ at about 100 cm). In contrast, the opposite trend would be advantageous for species having adult sizes in the range of 10–20 cm. For such animals, sculpture cannot become hydrodynamically useful until the adult size is attained (assuming *Nautilus* performance levels). Thus, formation of sculpture in the small, juvenile stages would require an investment of metabolic energy with no concomitant repayment of energy in the form of higher hydrodynamic efficiency (we assume here no non-hydrodynamic function for shell sculpture). With no hydrodynamic need to become rough until adult size is reached, these animals should remain smooth-shelled during their early growth stages and then become sculptured as maturity approaches. Since the hydrodynamic advantage of proper shell sculpture would be most important in good swimmers, these trends can be expected to be best developed in species with compressed shells (see Chamberlain's 1976 discussion of shell shape and swimming ability).

It is interesting to note that examples of such trends may be found among genera of many ammonite superfamilies including the Harpoceratacеae, Stephanocerataceae, Perisphinctaceae, Desmocerataceae, and Haploceratacеae. In these groups, many macroconchs (female dimorphs) with large involute, compressed shells are prominantly ribbed on the inner whorls but become smooth on the outer whorl. In contrast, many microconchs

(small shells of male dimorphs) become increasingly ornate on the outer whorl.

Tests of the Hydrodynamic Model

In the above paragraphs, we describe a model for the hydrodynamic functioning of shell sculpture in cephalopods. The main points of this model are: 1) the hydrodynamic effect of sculpture depends primarily on the size of the sculpture elements relative to the size of the shell, on their positions relative to one another and on the shell, and to swimming velocity; 2) sculpture is detrimental to swimming (reduces hydrodynamic efficiency) if it exceeds the height of the displacement layer; and 3) sculpture is advantageous to swimming (increases efficiency) if it remains within the boundary layer and induces premature conversion to turbulent boundary layer flow.

Our model can be tested on two levels. First, one can test the predictions we make about how sculpture affects drag coefficient. Two questions are important here: 1) does boundary layer conversion produce the drag coefficient decreases we describe (Figure 5); and 2) does shell sculpture produce drag coefficient changes similar to those observed in roughened cylinders (Figure 10)? Both questions can be resolved by obtaining drag coefficients from drag and velocity measurements on sculptured shells or shell models. This would require testing over a wide range of velocity and probably involve relatively sophisticated techniques of drag measurement (see Chamberlain 1976 for a description).

On the second, and perhaps more interesting level, one can examine whether fossil cephalopods actually used transition-related drag coefficient decreases to augment their swimming capabilities. This, of course, cannot be done directly since dead animals do not swim. But one can test the predictions of our model about: 1) change in the grade of shell sculpture with increasing shell size; and 2) change in sculpture dimensions as a function of position on the shell, velocity, etc. A positive result would be strong evidence for such usage and could give some insight into actual swimming velocities as well. Such work would involve measurement of shell sculpture size and location on individual shells and in ontogenetic series. This would best be done on species giving good evidence of being reasonably adept swimmers as these trends would be most important and thus best developed in them.

Function of Shell Sculpture

The function of cephalopod shell sculpture has been much discussed over the years, but no concensus and little quantitative evidence on the subject has yet developed. Spath (1919) has argued that ornament serves to strengthen the shell against implosion resulting from excessive hydrostatic pressure. Westermann (1971) doubts this and suggests that ornament may have been essentially protective in increasing the strength of the shell against impact or crushing by predators or in acting as camouflage. Cowen et al. (1973) have elaborated further on the idea that ornament acts as camouflage by arguing that it masks the regular outline of the shell. Teichert (1967) noted that some kinds of ornament are floored and hollow and thus proposed that they aided in buoyancy control. The importance of sculpture in swimming has been advanced by Spath (1919) who believed that keels increased streamlining; by Kummel & Lloyd (1955) who found that their "relative drag coefficient" tended to be high in strongly ribbed forms; by Westermann (1966) who studied the affect of intraspecific variation in whorl shape and ornamentation on streamlining and concluded that the high variation found in many species indicates low swimming activity; and now by us in our proposition that sculpture of the proper dimensions acting under the proper flow conditions augments swimming performance.

All the evidence is not yet in. Pronouncements on the subject are therefore unwarranted. But certain intimations seem clear. The widespread occurrence and morphologic variability of shell sculpture suggests a multiplicity of function; i.e. different functions in different species, or perhaps even in the same species. Beyond this, one conclusion appears inescapable. The mere presence of sculpture on a shell means that it must have had some hydrodynamic effect (as we show here) because it must have interacted with at least part of the flow past the shell. In poor swimmers this effect may well have been negligible, and the real function of sculpture may have lain elsewhere. But because of their critical need for energy conservation, reasonably adept

swimmers would have found any such effect most important. In such animals, we suspect that sculpture undoubtedly was designed primarily for hydromechanical purposes or at least, designed to perform some non-hydromechanical function in a way that would not adversely affect the hydrodynamic properties of the shell or swimming ability.

Summary

We have studied the hydrodynamic functioning of cephalopod shell sculpture by means of flow visualization experiments on sculptured shells and by applying drag coefficient data on simple geometric bodies to cephalopod shells. Our analysis suggests that:

1.) The main characteristics of flow structure in smooth shells are preserved in ornamented shells unless sculpture is large enough to extend through a shell's boundary layer. When this happens, vortices form behind protruding sculpture, break up the flow, greatly increase drag, and reduce swimming ability.

2.) The additional drag produced by shell sculpture depends on swimming velocity, shell size, and sculpture size and position on the shell. Nearly all drag-producing sculpture is located on the flanks of the leading part of the outer whorl. Sculpture on posterior surfaces or in the umbilicus has little hydrodynamic effect. In many species the most prominent sculpture is placed behind the lateral shoulder, where it has the least effect on the flow.

3.) In some ectocochliates, sculpture may have functioned to augment swimming capability by inducing premature boundary layer conversion in the manner of a roughened cylinder. Only sculpture within a narrow size range (generally less than about 0.5–2% shell diameter) will function in this way. Properly roughened shells may have conserved as much as 50% of the propulsive power required by smooth shells of the same size and shape (Figures 12 & 13). Species with compressed shells were more likely to have benefited from this phenomenon than other types.

4.) To be hydrodynamically optimal, sculpture must change in size during ontogeny. Species with small adult sizes ($\approx$ 10 cm) should become progressively more coarsely ornamented during growth, while species with large adult stages ($\approx$ 100 cm) should become progressively smoother. These allometries should be best developed in species with compressed shells and are observed among many ammonite genera.

5.) Cephalopod shell sculpture may have performed many functions in addition to that proposed here (3 of this summary). Nevertheless, the presence of sculpture on a shell means that it had some hydrodynamic effect. For many cephalopods, this effect was probably negligible, so that in this case, the function of sculpture was probably non-hydromechanical (e.g. camouflage, strength, etc.). But for others, it was undoubtedly of major importance and its function primarily hydrodynamic.

Acknowledgments

D. M. Raup (Univ. of Rochester) provided valuable advice during the course of this study. B. Latto (McMaster Univ.) allowed us to use his flume laboratory for our flow visualization experiments. D. Fisher (Univ. of Rochester), G. V. Middleton (McMaster Univ.), D. M. Raup, and P. Ward (McMaster Univ.) reviewed the manuscript. This work was done under a National Research Council of Canada operating grant to G.E.G.W., a National Research Council of Canada post-doctoral fellowship to J.A.C., and a Faculty Research Grant (#11433) from the Research Foundation of the City University of New York to J.A.C.

Literature Cited

ALEXANDER, R. McN. 1968. Animal Mechanics. 422 pp. Univ. of Washington Press; Seattle, Washington.

BAINBRIDGE, R. 1958. The speed of swimming of fish as related to size and to the frequency and amplitude of the tail beat. J. Exp. Biol. 35:109–133.

BAINBRIDGE, R. 1960. Speed and stamina in three fish. J. Exp. Biol. 37:129–153.

CADDY, J. F. 1968. Underwater observations on scallop (*Placopecten magellanicus*) behaviour and drag efficiency. J. Fish. Res. Board Can. 25:2123–2141.

CHAMBERLAIN, J. A., JR. 1971. Shell morphology and the dynamics of streamlining in ectocochliate cephalopods (abstr.). Geol. Soc. Am. Abstr. with Prog. 3:523–524.

CHAMBERLAIN, J. A., JR. 1973. Phyletic improvements in hydromechanical design and swimming ability in fossil nautiloids (abstr.). Geol. Soc. Am. Abstr. with Prog. 5:571–572.

CHAMBERLAIN, J. A., JR. 1976. Flow patterns and

drag coefficients of cephalopod shells. Palaeontology. *19*:539–563.

COLE, K. S. AND D. L. GILBERT. 1970. Jet propulsion in squid. Biol. Bull. *138*:245–246.

COWEN, R., R. GERTMAN, AND G. WIGGETT. 1973. Camouflage patterns in *Nautilus*, and their implications for cephalopod paleobiology. Lethaia. *6*: 201–214.

GERO, D. R. 1952. Power and efficiency of large salt water fish. Aeronaut. Eng. Rev., Jan. 1952. pp. 10–15.

GRAY, J. 1957. How fishes swim. Sci. Am. *197*: 48–53. [Reprinted in Readings From Scientific American: Oceanography. J. R. Moore, ed., 1971. pp. 228–234. W. H. Freeman; San Francisco, Calif.]

HERTEL, H. 1966. Structure, Form, and Movement. 251 pp. Reinhold; New York.

HOERNER, S. F. 1965. Fluid Dynamic Drag. 432 pp. Publ. by author; Midland Park, New Jersey.

JOHANNESSEN, C. L. AND J. A. HARDER. 1960. Sustained swimming speeds of dolphins. Science. *132*:1550–1551.

JORDAN, R. 1968. Zur Anatomie mesozoischer Ammoniten nach den Strukturelementen der Gehause-Innenwand. Beih. Geol. Jahrb. *77*:1–64.

KUMMEL, B. AND R. M. LLOYD. 1955. Experiments on relative streamlining of coiled cephalopod shells. J. Paleontol. *29*:159–170.

LANG, T. G. AND K. S. NORRIS. 1966. Swimming speed of a Pacific bottlenose porpoise. Science. *151*:558–590.

LEHMANN, U. 1971. New aspects in ammonite biology. Proc. North Am. Paleontol. Conv. Part I. pp. 1251–1269.

LEHMANN, U. 1972. Aptychen als Kieferelemente der Ammoniten. Paläontol. Z. *46*:34–48.

MAGNAN, A. 1930. Les characteristiques geometriques et physiques des poissons. Ann. Sci. Nat. Zool. Ser. 10. *13*:355–489.

MUTVEI, H. 1957. On the relations of the principle muscles to the shell in *Nautilus* and some fossil nautiloids. Ark. Miner. Geol. *2*:219–254.

MUTVEI, H. 1964. Remarks on the anatomy of recent and fossil cephalopoda. Stockholm Contrib. Geol. *11*:79–102.

PACKARD, A. 1969. Jet propulsion and the giant fibre response of *Loligo*. Nature. *221*:875–877.

PRANDTL, L. AND O. J. TIETJENS. 1934. Applied Hydro- and Aeromechanics. Dover ed. 311 pp. Dover, New York.

SPATH, L. F. 1919. Notes on ammonites. Geol. Mag. *56*:27–35, 65–74, 115–122, 170–177, 220–225.

STRINGHAM, E. 1924. Maximum speed of freshwater fishes. Am. Nat. *58*:156–161.

TEICHERT, C. 1967. Major features of cephalopod evolution. pp. 162–210. In: Teichert, C. and E. Yochelson, eds. Essays in Paleontology and Stratigraphy. Univ. of Kansas Press; Lawrence, Kansas.

TUCKER, V. A. 1975. The energetic cost of moving about. Am. Sci. *63*:413–419.

WESTERMANN, G. E. G. 1966. Covariation and taxonomy of the Jurassic Ammonite *Sonninia Adrica* (Waagen). Neues Jahrb. Geol. Paläontol., Abh. *124*:289–312.

WESTERMANN, G. E. G. 1971. Form, structure and function of shell and siphuncle in coiled Mesozoic ammonoids. Life Sci. Contrib., R. Ontario Mus. No. 78, 39 pp.